

Supplementary Data for

Creating MHC-restricted neoantigens with covalent inhibitors that can be targeted by immune therapy

Takamitsu Hattori^{1,2,4}, Lorenzo Maso^{1,4}, Kiyomi Y. Araki¹, Akiko Koide^{1,3}, James Hayman¹, Padma Akkapeddi¹, Injin Bang¹, Benjamin G. Neel^{1,3*}, Shohei Koide^{1,2*}

¹Laura and Isaac Perlmutter Cancer Center, New York University Langone Health, New York, NY.

²Department of Biochemistry and Molecular Pharmacology, New York University Grossman School of Medicine, New York, NY.

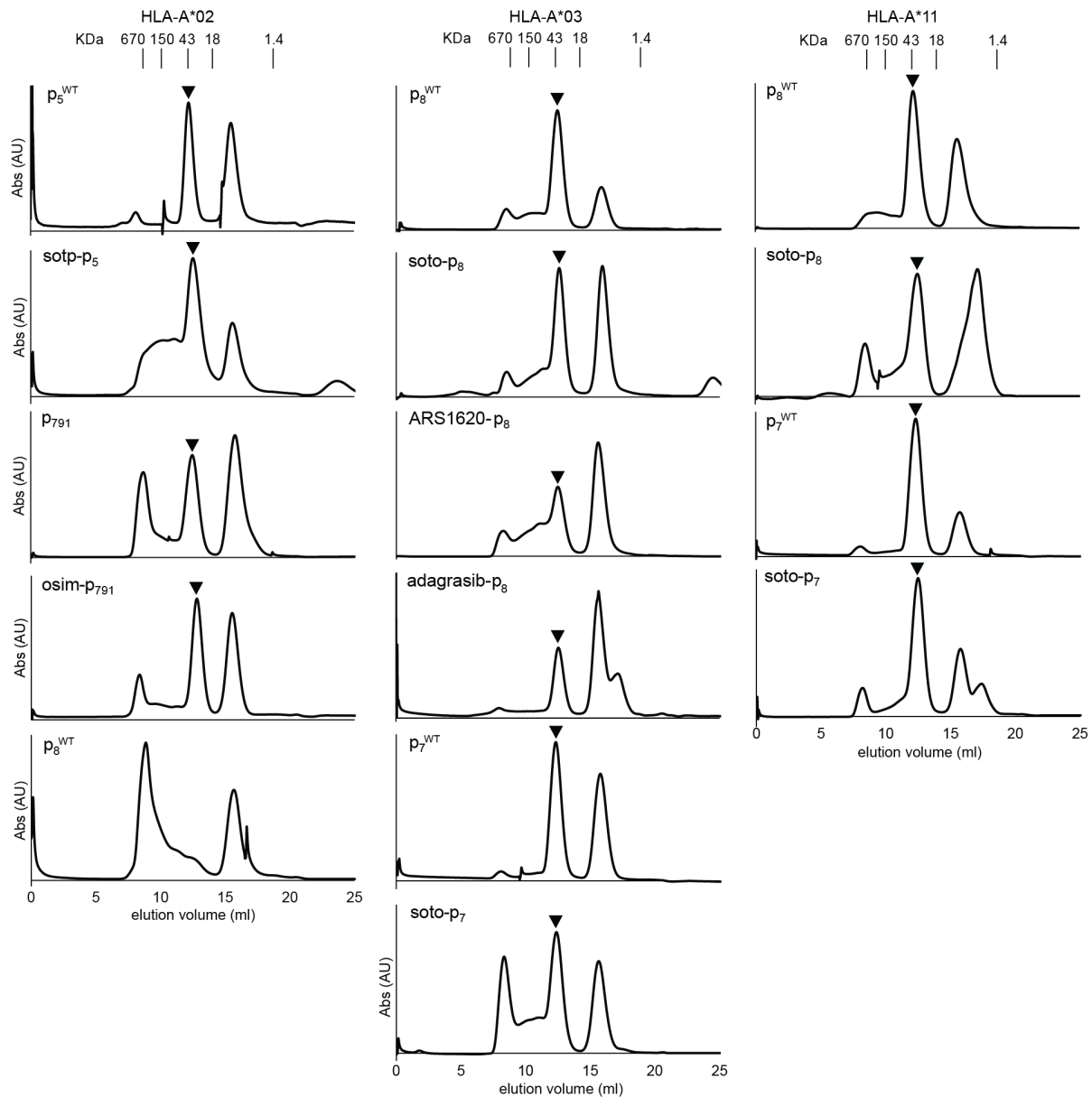
³Department of Medicine, New York University Grossman School of Medicine, New York, NY.

⁴Equal contribution.

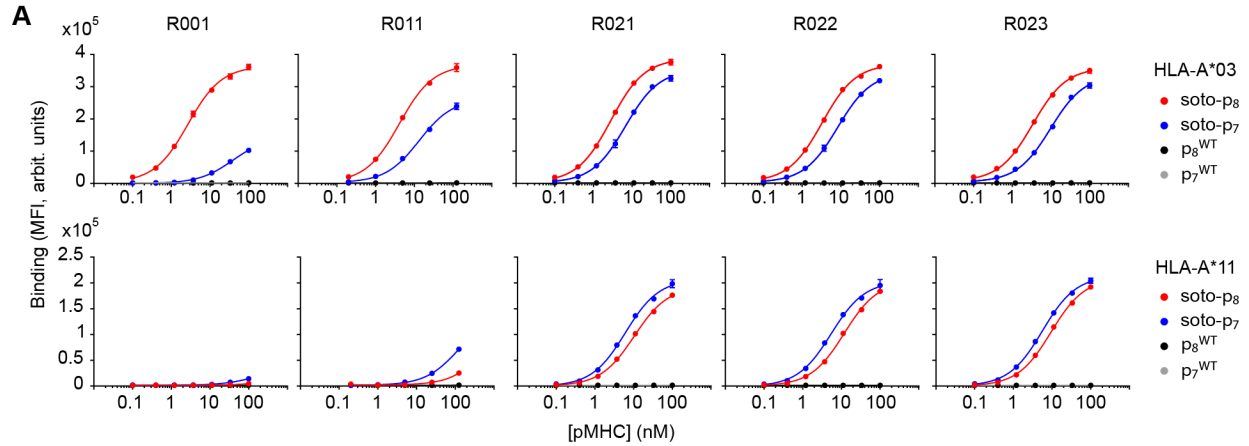
*Correspondence to Benjamin G. Neel and Shohei Koide

Email: Benjamin.Neel@nyulangone.org and Shohei.Koide@nyulangone.org

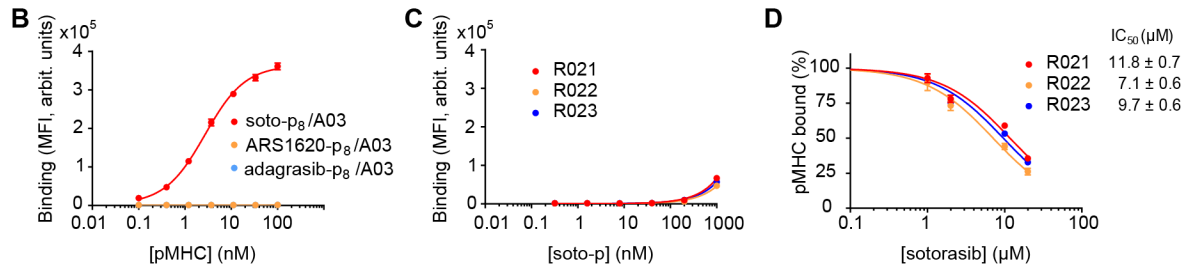
Supplementary Figures S1–S7



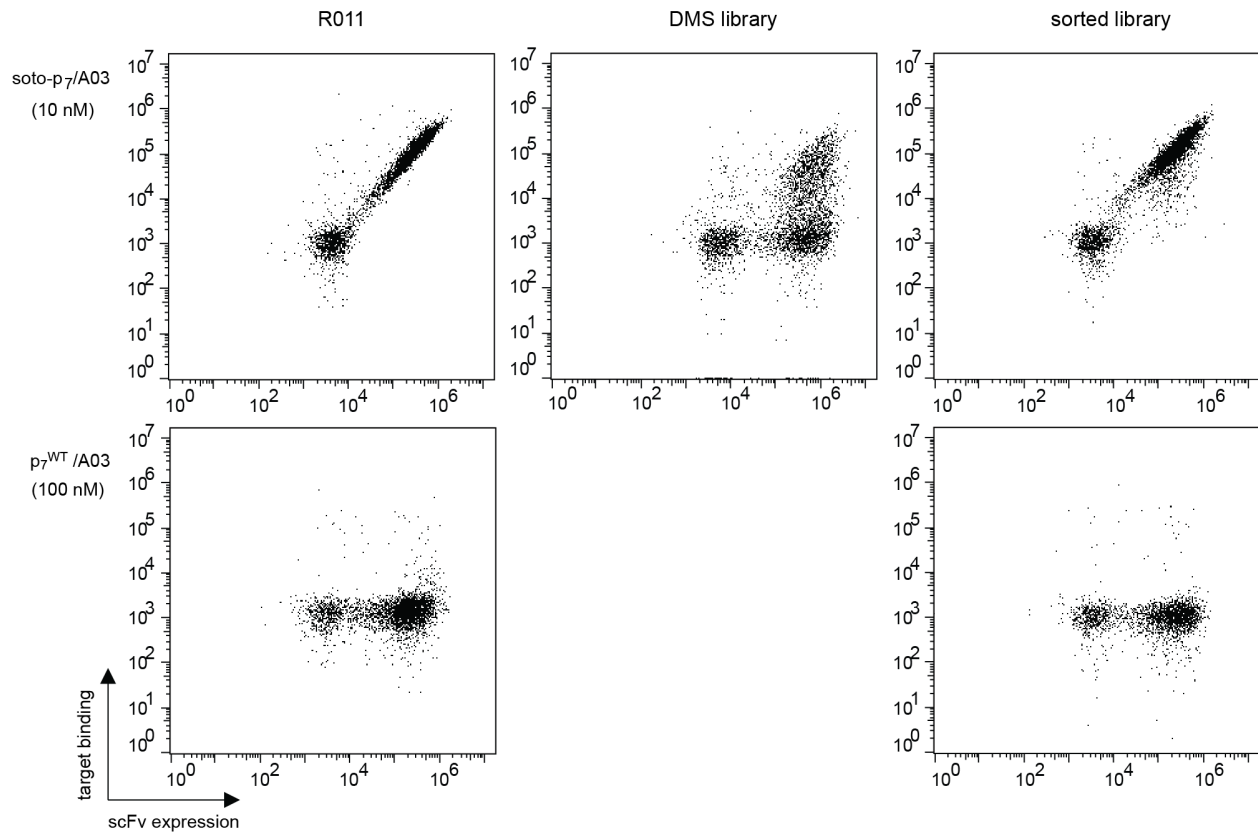
Supplementary Figure S1. Size exclusion chromatography profiles of products of the refolding reactions for p/MHCs utilized in this study. The curves show the absorbance at 280 nm of refolded p/MHC samples analyzed on a Superdex 75 10/300 GL in PBS. The black triangles, where present, indicate the peaks for the correctly assembled p/MHC complexes (~45 kDa), which were purified and used in this study. The vertical marks over each column indicate elution volumes of molecular weight standards run in the same conditions (thyroglobulin, 670 kDa; γ -globulin, 150 kDa; ovalbumin, 43 kDa; myoglobin, 17.6 kDa, and Vitamin B12, 1.35 kDa). The bottom panel on the left column shows the reaction of p_8 with HLA-A*02, a negative control, mismatched pair, which failed to reconstitute as expected.



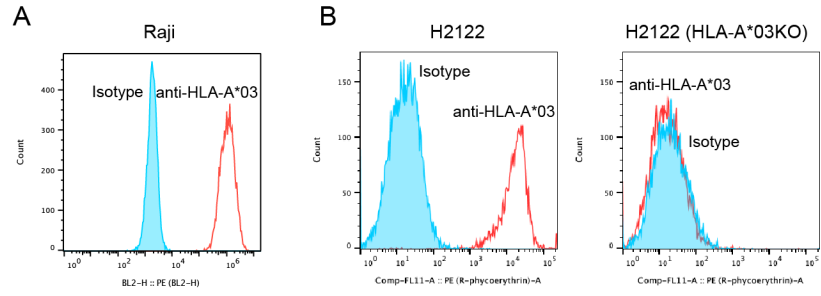
antigen	$K_{D, APP}$ (nM)				
	R001	R011	R021	R022	R023
soto-p ₈ /A03	2.7 ± 0.1	4.1 ± 0.4	2.8 ± 0.2	3.3 ± 0.1	3.4 ± 0.2
soto-p ₇ /A03	> 100	13.5 ± 2.0	6.7 ± 0.6	8.3 ± 0.6	9.8 ± 1.3
soto-p ₈ /A11	ND	ND	10.4 ± 0.5	11.8 ± 0.6	9.5 ± 0.9
soto-p ₇ /A11	ND	> 100	6.1 ± 0.3	5.5 ± 0.6	5.7 ± 0.2
p ^{WT} /MHCs	ND	ND	ND	ND	ND



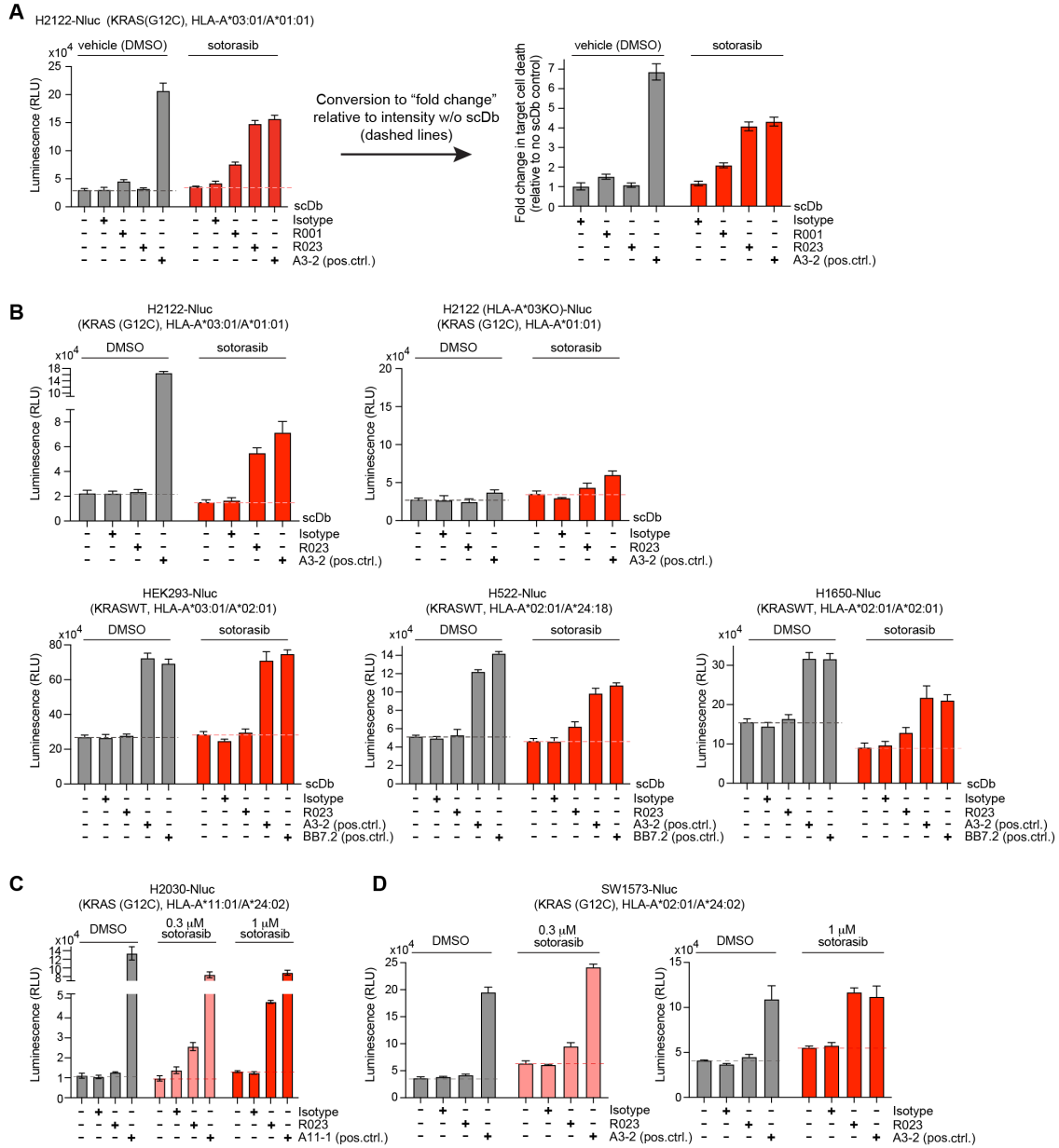
Supplementary Figure S2. Improvement of the binding properties of antibodies to sotorasib-KRAS(G12C) peptide conjugates in complex with MHCs over the course of the affinity maturation campaign. **(A)** Binding titrations of scFvs displayed on the yeast cell surface to the indicated pMHCs. Apparent K_D values mean \pm standard deviation ($n=3$, technical replicates) are shown in the table. ND, K_D value not determined, because the binding was too weak. **(B)** Binding titrations of R001 in the yeast display format to p₈ conjugated to different G12Ci molecules in complex with HLA-A*03. The data points for ARS1620-p₈/A03 (orange) and MRTX849-p₈/A03 (light blue) overlap nearly completely. **(C)** Binding titrations of R021 (red), R022 (orange), and R023 (blue) scFvs displayed on the yeast cell surface to a soto-peptide conjugate in the absence of MHC. **(D)** Competition by sotorasib of the interaction of soto-p₇/A03 (10 nM) with scFv R021 (red), R022 (orange), or R023 (blue) displayed on the yeast cell surface. The binding signals were normalized, with 100% signal corresponding to the signal in the absence of sotorasib and 0% signal corresponding to that in absence of soto-p₇/A03 or sotorasib. The IC_{50} values shown are the mean \pm s.d. ($n = 3$; technical replicates).



Supplementary Figure S3. Binding profiles soto-p7/A03 (top row) and p7^{WT}/A03 (bottom row) of clone R011 (left column), the naive deep mutational scanning library (middle column), and the pool after sorting for binding to soto-p7/A03 (right column) tested in the yeast-display format.

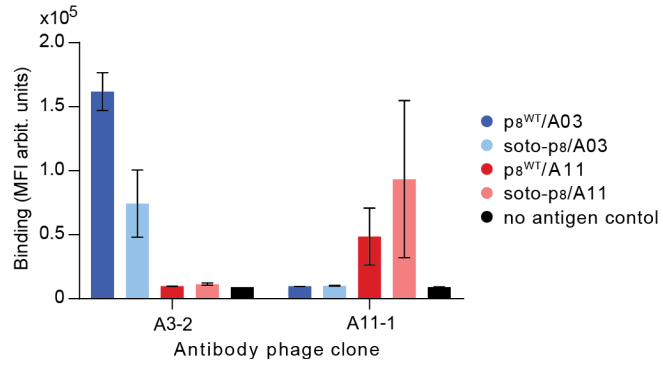


Supplementary Figure S4. HLA expression of cell lines. (A) Analysis of HLA-A*03 expression on Raji cells. (B) Analysis of HLA-A*03 expression on H2122 cells and H2122 (HLA-A*03KO) cells. Note the lack of HLA-A*03 in the latter, indicating that successful deletion.

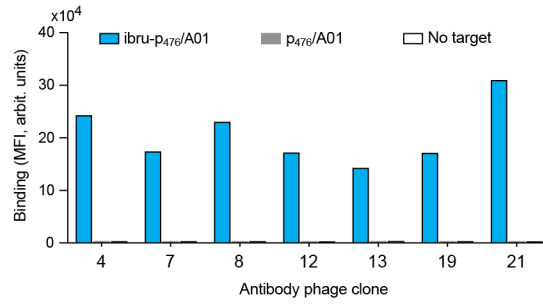


Supplementary Figure S5. Cytotoxic effects of the R023 scDb on sotorasib-treated tumor cells (A)

Conversion of luminescence intensity to normalized "fold change" relative to the intensity without scDb (the leftmost bar for each data set; also shown as dashed lines). The left graph is identical to Fig. 4C. Data sets with and without sotorasib pretreatment need to be separately normalized, because the numbers of cells at the end of cell killing assay, after 24 hr of coculture, differ for the two sets, leading to different absolute luminescence intensities. Thus, absolute luminescence intensities cannot be directly compared across different treatment schemes. Similarly, different cell lines express different levels of Nluc, and thus their absolute luminescence intensities cannot be directly compared. (B) Cytotoxic effects of the indicated scDbs on various tumor cell lines expressing NLuc treated with 0.3 μ M sotorasib. The scDb concentration was 1 nM. The dashed lines show the luminescence intensity without scDb, which were used as the references for signal normalization to generate Fig. 4F-4H. (C and D) Cytotoxic effect of the R023 scDb on H2030-Nluc cells (C) and SW1573-Nluc (D) treated with sotorasib. The scDb concentration was 1 nM. Anti-pan HLA-A*03/A*02 antibody (A3-2 scDb), anti-pan HLA-A*02 antibody (BB7.2 scDb), and anti-pan HLA-A*11 antibody (A11-1) were used as positive controls. Data shown are from quadruplicate measurements.



Supplementary Figure S6. Binding analysis of antibody phage clones to p/MHC complexes by the multiplex bead binding assay (MBBA). Phage MBBA signals showing the binding specificity of antibody clones (A3-2 and A11-1) that are not specific to the identity of the bound peptide.



Supplementary Figure S7. Binding analysis of antibody phage clones to ibru-p₄₇₆/A01 and p₄₇₆/A01 by the multiplex bead binding assay (MBBA). Phage MBBA signals showing the binding specificity of antibody clones against ibritinib-p₄₇₆/HLA-A*01.